Paramagnetic Mn impurities on Ge and GaAs surfaces

P. Gambardella and H. Brune
Institut de Physique des Nanostructures, Ecole Polytechnique Fédérale de Lausanne, CH-1015 Lausanne, Switzerland

S. S. Dhesi* and P. Bencok
European Synchrotron Radiation Facility, Boîte Postale 200, F-38043 Grenoble, France

S. R. Krishnakumar†
International Centre for Theoretical Physics (ICTP), Strada Costiera 11, I-34100 Trieste, Italy

S. Gardonio, M. Veronese, C. Grazioli, and C. Carbone
Istituto di Struttura della Materia, Consiglio Nazionale delle Ricerche, Area Science Park, I-34012 Trieste, Italy
(Received 26 February 2005; published 15 July 2005)

Individual Mn impurities deposited on Ge(100), Ge(111), and GaAs(110) substrates present magnetic moments significantly larger compared to the average Mn magnetization in bulklike $Ga_{1-x}Mn_xAs$ and Mn_xGe_{1-x} dilute magnetic semiconductors. The Mn magnetic moment is shown to change considerably going from Ge(100), to GaAs(110), and Ge(111). Independently of the substrate, the Mn *per atom* moment decreases with increasing coverage owing to the formation of antiferromagnetic Mn clusters. We observe no evidence of magnetically ordered surface layers down to a temperature of 5 K. The comparison of x-ray magnetic circular dichroism line shapes with that of a pure Mn d^5 configuration reveals the partial delocalization of the Mn *d* states.

DOI: 10.1103/PhysRevB.72.045337 PACS number(s): 75.50.Pp, 75.20.Hr, 78.70.Dm

The discovery of ferromagnetism in $Ga_{1-x}Mn_xAs$ (Ref. 1) and Mn_xGe_{1-x} (Ref. 2) semiconducting compounds with Curie temperature $T_C > 100$ K has fostered an intense research effort aimed at understanding and optimizing the mechanisms responsible for carrier-mediated magnetic order. The experimental situation is quite complex as both T_C and the saturation magnetization depend on the interplay of a variety of factors, which are ultimately determined by the growth conditions[3] and postgrowth annealing procedures.[4] The concentration and distribution of Mn dopants,[2,5] the carrier density,[2,5,6] the presence of common defects such as Mn interstitials,[7] Mn clusters,[5,8] and As antisites in $Ga_{1-x}Mn_xAs$ (Ref. 9) significantly influence the magnitude and sign of the magnetic coupling. As a result of this interplay, it is hard to find common ground to compare theoretical and experimental investigations and reach a consensus on the origin of the ferromagnetic properties of these compounds.[10] An example is the magnetization deficit that is found both in $Ga_{1-x}Mn_xAs$ (Refs. 11–16) and Mn_xGe_{1-x} (Ref. 2) when comparing the experimental saturation magnetization with that predicted on the basis of the Mn concentration and theoretical estimates of the Mn local moment. Deviations from the expected 4 μ_B (Refs. 17 and 18) and 3 μ_B (Refs. 2, 19, and 20) Mn moment in $Ga_{1-x}Mn_xAs$ and Mn_xGe_{1-x}, respectively, range from 20% to 80% in $Ga_{1-x}Mn_xAs$ (Refs. 11 and 12) and 45% to 60% in Mn_xGe_{1-x}.[2]

The aim of the present study is to explore GaMnAs and MnGe surface systems, where the presence of heterogeneous Mn phases and defects, particularly in the case of Ge, can be controlled to a better extent compared to thin films with typical thickness $\geqslant$10 nm addressed to this date. X-ray magnetic circular dichroism (XMCD) measurements performed on individual Mn impurities deposited on Ge(100) and GaAs(110) surfaces reveal spin moments close to that expected for paramagnetic Mn atoms and much larger than that typically detected in magnetically saturated $Ga_{1-x}Mn_xAs$ films.[12–15,21] Strong differences of the Mn magnetic moment are observed on Ge(100), Ge(111), and GaAs(110), emphasizing the role of the local coordination in determining the magnetization of Mn-doped semiconducting compounds. Moreover, we observe that the formation of Mn clusters is associated with a reduction of the magnetic moment per Mn atom due to antiferromagnetic Mn—Mn coupling. Finally, we found no evidence of two-dimensional long-range magnetic order in the investigated Mn concentration range.

The experiments were performed at beamline ID8 of the European Synchrotron Radiation Facility in Grenoble. Single crystal Ge(100), Ge(111), and GaAs(110) surfaces were prepared in ultrahigh vacuum by repeated Ar^+ sputtering and annealing cycles to 650 °C. The clean Ge(100) and Ge(111) surfaces showed the characteristic low energy electron diffraction (LEED) patterns of the (2×1) and $c(2\times8)$ reconstructions, respectively, in agreement with literature data.[22,23] GaAs(110) also showed the expected (110) LEED pattern,[24] but the precise stoichiometry of the surface remained undetermined, as preferential sputtering of As is likely to lead to Ga-rich surface layers. After cleaning, no surface oxidation was detected by x-ray absorption spectra (XAS) at the oxygen *K* edge. Mn atoms were deposited by means of an electron beam evaporator, calibrated by a quartz microbalance, at a temperature of 5 K to inhibit surface diffusion and subsequent cluster nucleation. The coverage is given in monolayers with respect to the bulk-truncated Ge(100) surface (1 ML$=6.2\times10^{14}$ atoms/cm^2). XAS was measured at the $L_{2,3}$ Mn edges in total electron yield mode using circularly and linearly polarized light with 99% ± 1% polarization in

magnetic fields of up to 6 T with the sample at $T=5$ K. XMCD was recorded by switching both the photon helicity and applied magnetic field **B** parallel to the surface normal.

Figure 1(a) shows the XAS spectra recorded for individual Mn atoms deposited on Ge(100), Ge(111), and GaAs(110) for parallel (I^+, solid lines) and antiparallel (I^-, dashed lines) alignment of the light helicity with $\mathbf{B}=6$ T. The pairs of XAS spectra are shown after normalization to the incident photon flux and to each other at 637 eV, and scaled to the same $I^+ + I^-$ intensity at the L_3 edge for comparison. Owing to the extremely small coverage, the Mn $L_{2,3}$ XAS is superposed to a noticeable background signal from the substrate. The latter, however, gives no contribution to the XMCD, as shown in Fig. 1(b). XAS and XMCD spectra are also reported for individual Mn atoms deposited on a K film and for a d^5 ground state calculated within a multiplet approach.[25] Transition metal impurities on alkali metal hosts are known to possess atomiclike ground states with full spin and orbital moment values.[26] The Mn/K spectra are henceforth used here for comparison, as representative of a pure Mn d^5 configuration in the present experimental conditions. This is justified also by the excellent agreement with the I^+, I^-, and $I^+ - I^-$ spectra calculated for an atomic d^5 ground state and by the Brillouin-like magnetization reported in Fig. 2(a).

The broadening of the multiplet features in the Mn/Ge(100), Ge(111), and GaAs(100) XAS and XMCD spectra compared to Mn/K reveals that the ground state of Mn atoms in contact with Ge and GaAs surfaces is not purely d^5 owing to varying degrees of hybridization of the impurity d states on different substrates, similarly to what is observed for submonolayer Mn films on metal surfaces.[27] This result is partly in contrast with previous XMCD studies on $Ga_{1-x}Mn_xAs$, where the XAS was interpreted in terms of d^4-d^5-d^6 configuration mixing, but the XMCD was assigned to an almost pure d^5 state by distinguishing for magnetic and nonmagnetic Mn species.[15,16] The magnitude of the XMCD effect relative to the XAS signal, however, shows that individual Mn impurities are strongly magnetic compared to Mn in $Ga_{1-x}Mn_xAs$ films, where a much smaller dichroism is observed.[12–15,21] The presence of Mn clusters, lattice defects, or Mn surface segregation and oxidation in thin films measurements is likely the cause of the reduced Mn moment in such systems, where these effects can be minimized by careful low-temperature annealing and HCl-surface etching.[16]

The different magnitude of the dichroic effect on Ge(100), Ge(111), and GaAs(110), observed by comparing I^+ and I^- [Fig. 1(a), inset] as well as $I^+ - I^-$ normalized by the total L_3 absorption intensity [Fig. 1(b)], indicates that the Mn magnetic moment changes on the three surfaces. In particular, it is largest on Ge(100) and progressively reduced on GaAs(110) and Ge(111). XMCD sum rules allow in principle to determine quantitatively the spin (m_S) and orbital (m_L) magnetic moments of metal atoms.[28] However, obtaining m_S for Mn and lighter $3d$ elements is not straightforward. In the case of Mn, the superposition of the $2p_{3/2}$ and $2p_{1/2}$ absorption edges leads to errors as large as 50% in the determination of m_S.[16,25] Further, m_S and m_L are proportional to $n_h/[\int(I_d^+ + I_d^-)dE]$, where n_h is the number of unoccupied Mn $3d$ states and $\int(I_d^+ + I_d^-)dE$ is the total intensity due to $2p \rightarrow 3d$ transitions, which requires subtraction of the $2p \rightarrow 3s$ signal from the measured XAS and, for very low Mn coverages as in Fig. 1, of the Ge or GaAs background. To circumvent these limitations, we note that the spectra of Mn/K

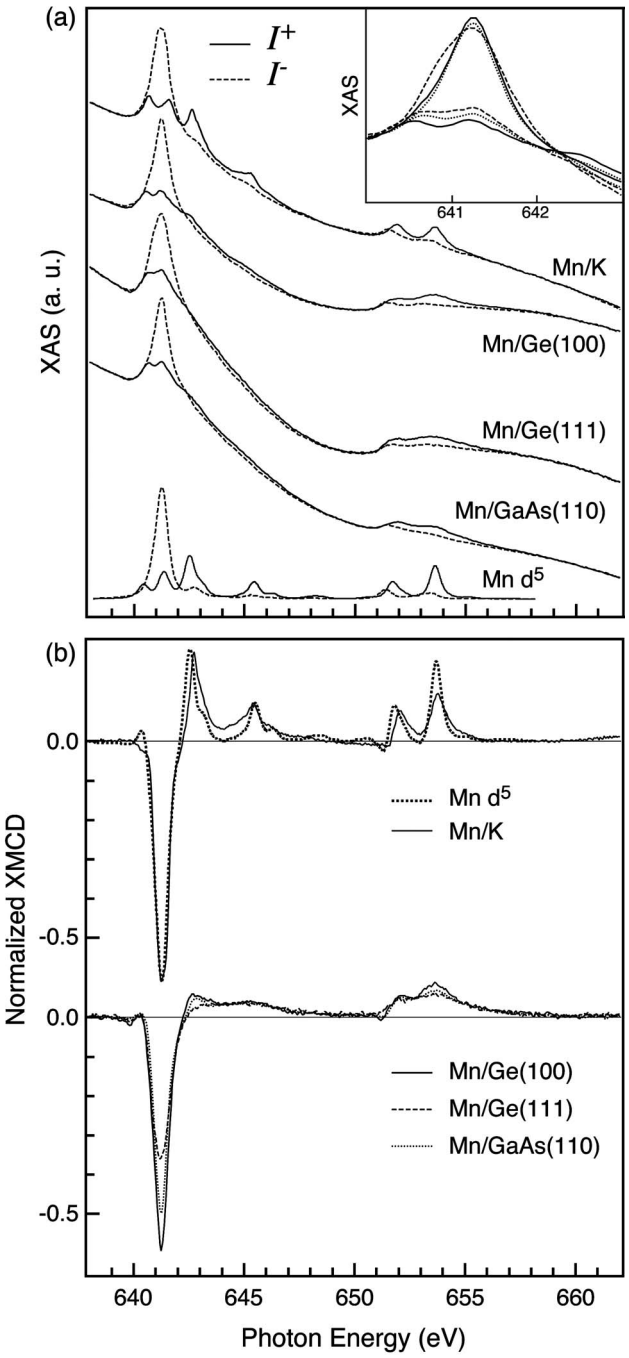

FIG. 1. (a) I^+, I^- spectra at the $L_{2,3}$ absorption edges of individual Mn impurities on K, Ge(100), Ge(111), and GaAs(110) surfaces. The Mn coverage is 0.01, 0.03, 0.02, 0.03 ML, respectively, $T=5$ K, $\mathbf{B}=6$ T. The inset shows a detail of I^+, I^- in the L_3 region for Mn/Ge(100) (solid lines), Mn/Ge(111) (dotted lines), and Mn/GaAs(110) (dashed lines). (b) $I^+ - I^-$ spectra scaled to the integrated $I^+ + I^-$ intensity over the L_3 edge. Calculations for I^+, I^-, and $I^+ - I^-$ are also shown for $2p^6 3d^5 \rightarrow 2p^5 3d^6$ transitions of a fully spin-polarized d^5 atomic ground state in the limit of zero crystal field and $T=5$ K.

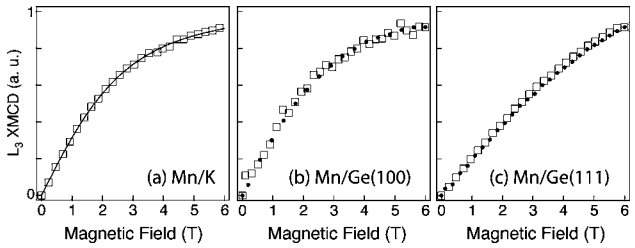

FIG. 2. Magnetization of (a) Mn/K as a function of applied field (squares), 0.01 ML Mn. The solid line represents a Brillouin function with $L=0$, $S=J=2.5$. (b) Mn/Ge(100) 0.006 ML (squares) and 0.12 ML (dots). (c) Mn/Ge(111) 0.09 ML (squares) and 0.18 ML (dots). $T=5$ K in all cases.

correspond precisely to a configuration with $m_S=5\ \mu_B$ and $m_L=0\ \mu_B$. We then calculate m_S as given by the XMCD sum rules by approximating $\int(I_d^+ + I_d^-)dE$ with the area comprised under the $I^+ + I^-$ spectrum between 639 and 647 eV, using a linear background subtraction. For Mn/K this gives a multiplicative correction factor of about 1.8 to obtain the expected m_S value at $T=5$ K, $\mathbf{B}=6$ T. This factor is then applied to Mn on Ge(100), Ge(111), and GaAs(110) yielding $m_S=4.8$, 3.3, and 4.0 μ_B, respectively. These numbers are within ±5% of those obtained by other background subtraction methods. Here, we have assumed $n_h=5$ in all cases, which might overestimate m_S by as much as 6% for the lowest estimate n_h

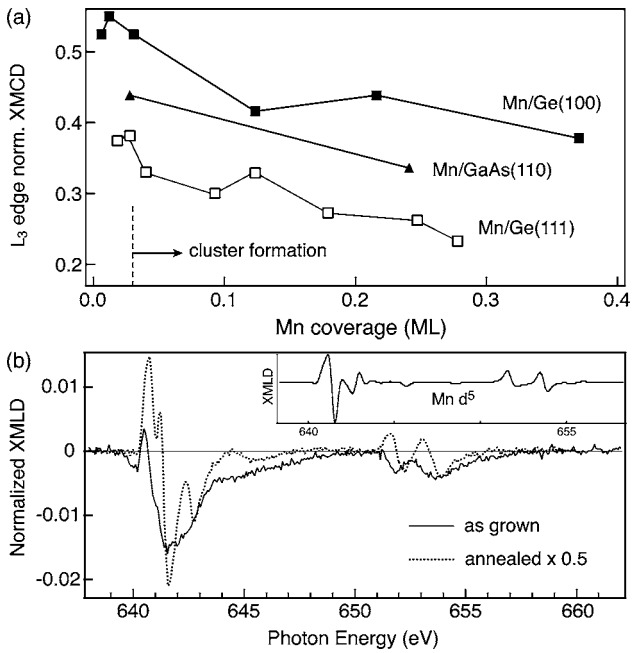

FIG. 3. (a) $(I^+ - I^-)/(I^+ + I^-)$ XMCD intensity at the L_3 edge as a function of Mn coverage at $T=5$ K, $\mathbf{B}=6$ T. (b) XMLD spectra normalized by the total L_3 XAS measured by switching between vertical and horizontal polarized light with the sample rotated about the vertical axis by 60° relative to $\mathbf{B}$ and the beam incidence direction. The solid line spectrum is obtained for 0.10 ML Mn/Ge(111) at $T=5$ K, $\mathbf{B}=6$ T. Annealing the sample to 150 °C results in stronger XMLD with remanent alignment at $T=5$ K, $\mathbf{B}=0$. The inset shows the calculated XMLD spectra for atomic Mn in an ideal 90° geometry.

=4.7 found in the literature.[17,18] This effect, however, is partly compensated by the fact that the paramagnetic Mn moments are not fully aligned parallel to $\mathbf{B}$ at 6 T and $T=5$ K, so that the saturation Mn moment is underestimated by about 5% and 10% for GaAs(110) and Ge(111), respectively. Taking into account the different uncertainty factors, we therefore put an overall accuracy limit of ±10% on the reported m_S.

Whereas m_S for Mn/GaAs(110) is close to the predicted 3.7–4.0 μ_B (Refs. 17 and 18) and to the value of 4.5 μ_B recently derived by XMCD in Ref. 16, m_S on Ge surfaces is significantly larger than the 1.4–1.9 μ_B measured for Mn_xGe_{1-x}.[2] *Ab initio* calculations for bulk Mn_xGe_{1-x} consistently indicate $m_S=3\ \mu_B$ and an $e_g^2(\uparrow)t_{2g}^2(\uparrow)t_{2g}^1(\downarrow)$ Mn configuration[2,19,20] arising from strong hybridization with the Ge 4p states. Very interestingly, while the moment of Mn/Ge(111) is in good agreement with that calculated for bulk impurities in Ge (Refs. 2, 19, and 20) and on Ge(111),[29] Mn/Ge(100) presents a much larger m_S. This difference is attributed to the local coordination of Mn atoms on Ge(111) and Ge(100).[30] In particular, the presence of dangling bonds on the $c(2\times 8)$ reconstructed Ge(111) surface is likely to lead to stronger hybridization between the Mn 3d and Ge 4p states compared to Ge(100), and to the concomitant reduction of m_S. We note also that small but positive m_L (parallel to m_S) are observed, about 0.07 μ_B for Mn/Ge(100) and Mn/GaAs(110) and 0.13 μ_B for Mn/Ge(111). The latter larger deviation from the ideal d^5 case with $m_L=0$ is consistent with the increased hybridization and related broadening of the Mn/Ge(111) XAS and XMCD features relative to Mn/Ge(100) and Mn/GaAs(110) [see inset in Figs. 1(a) and 1(b)]. Only very weak differences are detected between the in-plane and out-of-plane Mn magnetization, in agreement with the small magnetic anisotropy expected for such low values of m_L.[31] Finally, we remark that different adsorption sites on each surface can be occupied by Mn, but that site-dependent magnetic moments cannot be distinguished in the present study. Both scanning tunneling microscopy and theoretical investigations, however, indicate a strong preference for hollow adsorption sites on Ge(111) and Ge(100),[29,30,32] whereas large diffusion barriers prevent Mn to reach subsurface sites at low temperature.

We have further investigated the possibility of achieving ferromagnetism limited to one or a few surface atomic layers as a function of Mn concentration, an issue of fundamental as well as practical interest to control spin-polarized electron transport across heterogeneous interfaces. We remark that ferromagnetic coupling would be expected in a Ruderman–Kittel–Kasuya–Yosida picture of hole-mediated ferromagnetism and that the radial decay of the impurity-impurity oscillatory interaction changes from $1/r^{-3}$ in the bulk to $1/r^{-2}$ in a two-dimensional surface system.[33] Here, however, all samples with coverage in the range 0.006–0.35 ML display paramagnetic behavior [Figs. 2(b) and 2(c)], independently of their extrinsic bulk doping (2×10^{18} cm^{-3} n-doped Ge and GaAs, and 2×10^{19} cm^{-3} p-doped Ge) and despite the fact that Mn impurities typically act as acceptors in these materials. The absence of magnetic coupling even for relatively high Mn concentrations compared to bulk ferromag-

netic $Ga_{1-x}Mn_xAs$ and Mn_xGe_{1-x} is attributed to the different electrical properties of bulk and surface semiconductors and, tentatively, to a low carrier/dopant yield, as also observed for δ-doped Mn layers in GaAs.[34]

Increasing the Mn coverage at temperatures below the surface diffusion threshold leads initially to randomly distributed Mn impurities with increasing concentration and eventually to the statistical formation of Mn clusters of increasing size. We observe that the formation of Mn metal clusters as a function of coverage is accompanied by the decrease of the XAS-normalized XMCD signal [Fig. 3(a)], which indicates a reduced magnetic moment per Mn atom relative to individual impurities. Similar effects have been observed in $Ga_{1-x}Mn_xAs$ by increasing the Mn concentration and tentatively attributed to the formation of MnAs clusters.[11] In the present case, we show that partial or frustrated antiferromagnetic alignment in Mn clusters is the cause of the observed magnetization reduction. While XMCD is proportional to the scalar product of the magnetization with the photon helicity direction, x-ray magnetic linear dichroism (XMLD) is proportional to the square module of the magnetization and, hence, sensitive to both ferromagnetic and antiferromagnetic alignment. XMLD spectra were recorded with $\mathbf{B}=6$ T in order to align the Mn uncompensated spins close to one of the two orthogonal linear polarization directions. A typical spectrum is reported for 0.25 ML Mn/Ge(111) in Fig. 3(b) (solid line). We find that, while the XMCD decreases, the XMLD signal stays constant or increases weakly with Mn coverage, indicating a growing ratio of antiferromagnetic to ferromagnetic Mn species on the surface. Finally, annealing Mn/Ge(111) to 150 °C results in larger clusters that show remanent antiferromagnetic behavior (dotted line).

We wish to thank Kenneth Larsson and Gilles Retout for their assistance during the experiment, Riccardo Gusmeroli and Claudia Dallera for useful discussions and for making available to us their version of the atomic multiplet calculation code of Cowan, Butler, and Thole.[27] We also thank Tien-Lin Lee for supplying us with one of the Ge samples. This work has been supported by the Swiss National Science Foundation (project No. 21–63864) and the Italian Ministero dell'Istruzione, dell'Università e della Ricerca (FIRB project "Nanotecnologie e nanodispositivi optoelettronici, elettronici e spintronici").

*Present address: Diamond Light Source, Chilton, Didcot, UK.
†Present address: Surface Physics Division, Saha Institute of Nuclear Physics, Kolkata, India.

[1] H. Ohno, A. Shen, F. Matsukura, A. Oiwa, A. Endo, S. Katsumoto, and Y. Iye, Appl. Phys. Lett. **69**, 363 (1996).
[2] Y. D. Park, A. T. Hanbicki, S. C. Erwin, C. S. Hellberg, J. M. Sullivan, J. E. Mattson, T. F. Ambrose, A. Wilson, G. Spanos, and B. T. Jonker, Science **295**, 651 (2002).
[3] H. Shimizu, T. Hayashi, T. Nishinaga, and M. Tanaka, Appl. Phys. Lett. **74**, 398 (1999).
[4] T. Hayashi, Y. Hashimoto, S. Katsumoto, and Y. Iye, Appl. Phys. Lett. **78**, 1691 (2001).
[5] S. J. Potashnik, K. C. Ku, J. J. Berry, S. H. Chun, N. Samarth, and P. Schiffer, Appl. Phys. Lett. **79**, 1495 (2001).
[6] B. Beschoten, P. A. Crowell, I. Malajovich, D. D. Awschalom, F. Matsukura, A. Shen, and H. Ohno, Phys. Rev. Lett. **83**, 3073 (1999).
[7] K. M. Yu, W. Walukiewicz, T. Wojtowicz, I. Kuryliszyn, X. Liu, Y. Sasaki, and J. K. Furdyna, Phys. Rev. B **65**, 201303(R) (2002).
[8] Y. D. Park, A. Wilson, A. T. Hanbicki, J. E. Mattson, T. Ambrose, G. Spanos, and B. T. Jonker, Appl. Phys. Lett. **78**, 2739 (2001).
[9] K. W. Edmonds, P. Boguslawski, K. Y. Wang, R. P. Campion, S. N. Novikov, N. R. S. Farley, B. L. Gallagher, C. T. Foxon, M. Sawicki, T. Dietl, M. B. Nardelli, and J. Bernholc, Phys. Rev. Lett. **92**, 037201 (2004).
[10] See, e.g., T. Dietl and H. Ohno, MRS Bull. **28** (10), 714 (2003), and references therein.
[11] S. J. Potashnik, K. C. Ku, R. Mahendiran, S. H. Chun, R. F. Wang, N. Samarth, and P. Schiffer, Phys. Rev. B **66**, 012408 (2002).
[12] H. Ohldag, V. Solinus, F. U. Hillebrecht, J. B. Goedkoop, M. Finazzi, F. Matsukura, and H. Ohno, Appl. Phys. Lett. **76**, 2928 (2000).
[13] S. Ueda, S. Imada, T. Muro, Y. Saitoh, S. Suga, F. Matsukura, and H. Ohno, Physica E (Amsterdam) **10**, 210 (2001).
[14] Y. L. Soo, G. Kioseoglou, S. Kim, X. Chen, H. Luo, Y. H. Kao, H.-J. Lin, H. H. Hsieh, T. Y. Hou, C. T. Chen, Y. Sasaki, X. Liu, and J. K. Furdyna, Phys. Rev. B **67**, 214401 (2003).
[15] K. W. Edmonds, N. R. S. Farley, R. P. Campion, C. T. Foxon, B. L. Gallagher, T. K. Johal, G. van der Laan, M. MacKenzie, J. N. Chapman, and E. Arenholz, Appl. Phys. Lett. **84**, 4065 (2004).
[16] K. W. Edmonds, N. R. S. Farley, T. K. Johal, G. van der Laan, R. P. Campion, B. L. Gallagher, and C. T. Foxon, Phys. Rev. B **71**, 064418 (2005).
[17] Y.-J. Zhao, W. T. Geng, K. T. Park, and A. J. Freeman, Phys. Rev. B **64**, 035207 (2001).
[18] P. Mahadevan and A. Zunger, Phys. Rev. B **69**, 115211 (2004), and references therein.
[19] A. Stroppa, S. Picozzi, A. Continenza, and A. J. Freeman, Phys. Rev. B **68**, 155203 (2003).
[20] Y.-J. Zhao, T. Shishidou, and A. J. Freeman, Phys. Rev. Lett. **90**, 047204 (2003).
[21] D. J. Keavney, D. Wu, J. W. Freeland, E. Johnston-Halperin, D. D. Awschalom, and J. Shi, Phys. Rev. Lett. **91**, 187203 (2003).
[22] S. D. Kevan, Phys. Rev. B **32**, 2344 (1985).
[23] D. J. Chadi and C. Chiang, Phys. Rev. B **23**, 1843 (1981).
[24] P. Skeath, W. A. Saperstein, P. Pianetta, I. Lindau, W. E. Spicer, and P. Mark, J. Vac. Sci. Technol. **15**, 1219 (1978).
[25] G. van der Laan and B. T. Thole, Phys. Rev. B **43**, 13 401 (1991).
[26] P. Gambardella, S. S. Dhesi, S. Gardonio, C. Grazioli, P. Ohresser, and C. Carbone, Phys. Rev. Lett. **88**, 047202 (2002).
[27] H. A. Durr, G. van der Laan, D. Spanke, F. U. Hillebrecht, and N. B. Brookes, Phys. Rev. B **56**, 8156 (1997).

[28] C. T. Chen, Y. U. Idzerda, H.-J. Lin, N. V. Smith, G. Meigs, E. Chaban, G. H. Ho, E. Pellegrin, and F. Sette, Phys. Rev. Lett. **75**, 152 (1995).
[29] G. Profeta, S. Picozzi, A. Continenza, and C. Franchini, Phys. Rev. B **70**, 155307 (2004).
[30] W. Zhu, H. H. Weitering, E. G. Wang, E. Kaxiras, and Z. Zhang, Phys. Rev. Lett. **93**, 126102 (2004).
[31] P. Gambardella, S. Rusponi, M. Veronese, S. S. Dhesi, I. Cabria, R. Zeller, P. H. Dederichs, A. Dallmeyer, C. Grazioli, K. Kern, C. Carbone, and H. Brune, Science **300**, 1130 (2003).
[32] C. Zeng, W. Zhu, S. C. Erwin, Z. Zhang, and H. H. Weitering, Phys. Rev. B **70**, 205340 (2004).
[33] B. Fischer and M. W. Klein, Phys. Rev. B **11**, 2025 (1975).
[34] A. M. Nazmul, S. Sugahara, and M. Tanaka, Appl. Phys. Lett. **80**, 3120 (2002).